Biosensors and Bioelectronics 59 (2014) 14–20

Contents lists available at ScienceDirect

Biosensors and Bioelectronics

journal homepage: www.elsevier.com/locate/bios

Enzyme-induced modulation of the emission of upconverting nanoparticles: Towards a new sensing scheme for glucose

Melisa del Barrio [a,b,c], Susana de Marcos [c], Vicente Cebolla [b], Josef Heiland [a], Stefan Wilhelm [a], Thomas Hirsch [a], Javier Galbán [c,*]

[a] Institute of Analytical Chemistry, Chemo- and Biosensors, University of Regensburg, 93040 Regensburg, Germany
[b] Group of Chemical Technology for Separation and Detection, Instituto de Carboquímica – CSIC, 50018 Zaragoza, Spain
[c] Analytical Biosensors Group (GBA), Analytical Chemistry Department, Faculty of Science, Aragon Institute of Nanoscience (INA), University of Zaragoza, 50018 Zaragoza, Spain

ARTICLE INFO

Article history:
Received 27 November 2013
Received in revised form
26 February 2014
Accepted 27 February 2014
Available online 18 March 2014

Keywords:
Upconverting nanoparticles
Glucose biosensor
Near-infrared excitation
Glucose oxidase

ABSTRACT

A new approach for the design of a fluorometric biosensor for continuous monitoring of glucose levels in biological samples based on near-infrared (NIR) excitation is described. The sensor combines the fluorescence of the enzyme glucose oxidase (GOx) chemically modified with a fluorescein derivative (FS) and the luminescent properties of upconverting luminescent nanoparticles (UCLNPs). Both, the chemically modified enzyme (GOx-FS) and the UCLNPs are immobilized in a poly(acrylamide) film as a physical support. The excitation of the UCLNPs with NIR light is of major advantage, since fluorescence background from the matrix is minimized. The upconverted luminescence is used to excite GOx-FS, which undergoes a change in the fluorescence intensity during the enzymatic reaction with glucose. The sensor comprises sufficient stability and covers the physiological range of glucose levels in blood. Furthermore, in a proof of principle experiment, the sensor system responds linearly to glucose concentrations in the range from 3.3 to 16.6 mM in flow injection analysis mode.

1. Introduction

The synthesis and application of photon-upconverting luminescent nanoparticles (UCLNPs) have gained considerable interest because they exhibit outstanding photo-physical properties which make them highly attractive for applications in optical sensing, especially for biological samples whose autofluorescence under shortwave excitation represents a serious problem (Cheng et al., 2013; Gorris and Wolfbeis, 2013; Shen et al., 2013; Wang et al., 2010a). The phenomenon of upconversion luminescence was first investigated in rare earth-doped bulk materials by Auzel, Ovsyankin, and Feofilov (Auzel, 2004). It is characterized by the conversion of low energy excitation light into high energy emissions by an anti-Stokes process (Haase and Schafer, 2011). The excitation energy, usually near-infrared (NIR) light, is absorbed by a sensitizer ion (e.g., Yb^{3+}) and sequentially transferred to an activator ion (e.g., Er^{3+} or Tm^{3+}) via a non-radiative, resonant energy transfer process (Wang and Liu, 2009). The combined energies of pump photons are stored in metastable, long-lived energy states of the f-element ions (Ye et al., 2010). Thus, energy transfer upconversion (ETU) can take place and can lead to the emission of a photon of higher energy (f–f transition) (Menyuk et al., 1972). UCLNPs offer several advantages over commonly used fluorophores such as semiconductor quantum dots, organic fluorophores, or multiphoton excitation employing fluorescent (organic) dyes with Stokes-shifted emissions: (1) UCLNPs display narrow emission bands and the wavelengths are tunable by proper choice of dopant ions. (2) UCLNPs can be excited with low power NIR light, usually a continuous-wave (CW) laser. (3) The autofluorescence background of biological samples is low. (4) The penetration length of NIR light into tissue is much higher than that of shorter wave light. (5) Photodamage in biological systems by NIR light is negligible. (6) UCLNPs do not blink and show no photobleaching (Chan et al., 2012; Park et al., 2009; Wang et al., 2010b; Wu et al., 2009; Xu et al., 2013). All these advantages of UCLNPs together offer a very promising platform for their application to optical bio-sensing.

The development of optical (bio)sensors for the noninvasive monitoring of glucose in human fluids is undoubtedly a hot-topic in scientific research (Steiner et al., 2011; Tuchin, 2009). In this context, one of the most interesting lines of work is based on the fact that glucose concentration in interstitial fluids is related to the blood glucose concentration (Jin et al., 2011; Weidemaier et al., 2011).

* Corresponding author.
E-mail address: jgalban@unizar.es (J. Galbán).

http://dx.doi.org/10.1016/j.bios.2014.02.076
0956-5663/

According to this, optical (bio)sensors can be designed to be constituted by a fluorescent (bio)chemical receptor which reversibly reacts with glucose, implanted under the skin; its fluorescence is non-invasively monitored by exciting and detecting fluorescence from the outside of the epidermis. Several (bio)chemicals can be used as reversible receptors, enzymes being very well positioned compared to other biological macromolecules as antibodies or transport proteins (Galban et al., 2012). The main limitation associated with enzymes is their lack of adequate optical properties which forces to the use of an indicator (fluorescent or colorimetric) for the enzymatic reaction; since most indicators irreversibly change along the enzymatic reaction, the global reversibility of the sensor is lost. Fortunately, some kinds of enzymes, mainly flavoenzymes (Silva and Edwards, 2006) containing flavin adenine dinucleotide (FAD), present spectroscopic properties, which are still being studied (Kao et al., 2008), and they can be used as the starting point for being successfully implemented in optical continuous monitoring systems (OCMS) for clinical samples. Glucose oxidase (GOx) belongs to this group.

It is very well known that the spectroscopic properties of FAD depend on its oxidation state and the surrounding environment. When it is free in solution, the molecular absorption of FAD (at 375 and 450 nm) is weak but stronger than that of $FADH_2$, and the weak fluorescence of FAD (at 520 nm) almost disappears for $FADH_2$. In GOx containing FAD, its molecular absorption properties remain but its fluorescence nearly disappears, so it is very difficult to use the autoindicating intrinsic properties of GOx in optical sensors. Several strategies have been proposed for overcoming this problem (De Luca et al., 2007). One consists in the chemical linkage of a fluorophore able to produce energy transfer or to suffer the differential inner filter effect caused by FAD/$FADH_2$. In this sense, fluorescein (FS) (Sanz et al., 2003) and pyrene (Tatsu and Yamamura, 2002) have been successfully linked to GOx (GOx-FS). This permits the GOx-FS to be used in OCMS (see Supporting information: GOx-FS as a glucose biosensor).

Here, we report on a novel approach to modulate the blue emission of UCLNPs for the design of a fluorometric (bio)sensor for continuous monitoring of glucose levels in biological samples based on NIR excitation. The sensor system consists of a chemically modified enzyme (GOx-FS) and UCLNPs, which are embedded within a poly(acrylamide) film. The UCLNPs act as nanolamps and excite GOx-FS, which shows an emission at 520 nm due to FS fluorescence (Fig. 1). GOx-FS undergoes a change in its fluorescence intensity during the enzymatic reaction with glucose in the steady state equilibrium. This change can be related to the glucose concentration.

2. Materials and methods

2.1. Chemicals

Yttrium(III) chloride hexahydrate (99.99%), ytterbium(III) chloride hexahydrate (99.9%), thulium(III) chloride hexahydrate (99.99%), ammonium fluoride (ACS reagent ≥98.0%), sodium hydroxide (reagent grade ≥98.0%), 6-[fluorescein-5(6)-carboxamido]hexanoic acid N-hydroxysuccinimide ester (FS), glucose oxidase from *Aspergillus niger* (type X-S, lyophilized powder, with an activity of 147.9 U mg^{-1} of lyophilized solid, EC 1.1.3.4), β-D(+)-glucose, sodium hydrogencarbonate, sodium carbonate, 2-(N-morpholino)ethanesulfonic acid (MES), acrylamide, N,N′-methylenebisacrylamide, ammonium persulfate and Sephadex® G-50 were purchased from Sigma-Aldrich (Germany). N,N,N′,N′-tetramethylethylenediamine (TEMED) was purchased from BioRad (USA). Oleic acid (technical grade 90%) and 1-octadecene (technical grade 90%) were from Alfa Aesar (Germany). DSPE-mPEG(2000) (1,2-distearoyl-*sn*-glycero-3-phosphoethanolamine-N-[methoxy(polyethylene glycol)-2000] (ammonium salt)) was purchased from Avanti Polar Lipids (USA). All other reagents and organic solvents were of the highest grade available and used without further purification.

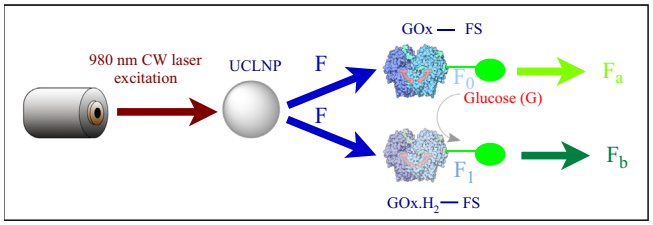

Fig. 1. Schematic drawing of the sensor concept. The UCLNPs act as nanolamps (upconversion luminescence upon 980 nm laser excitation) and excite GOx-FS, which undergoes a change in fluorescence during the enzymatic reaction with glucose. This change (F_b/F_a) can be related to the glucose concentration.

2.2. Instrumentation

We used the Zetasizer Nano-ZS from Malvern (UK) for DLS (Dynamic Light Scattering) experiments. Transmission electron microscopy (TEM) was performed using a 120 kV Philips CM12 microscope (FEI, The Netherlands). The size distributions of the corresponding nanoparticles were evaluated from the TEM images using the ImageJ software (USA). For the preparation of the UCLNPs all centrifugation steps were carried out with a Hettich Universal 320 centrifuge (Germany) and a Sonorex Digitech DT255H ultrasonic bath from Bandelin (Germany) was used. X-ray powder diffraction (XRD) patterns with a resolution of 0.005° (2θ) were collected using a Huber Guinier G670 diffractometer (Huber, Germany) with a Cu source (Kα radiation, $\lambda = 1.54060$ Å) operating at 40 kV and 30 mA. The upconversion luminescence lifetimes were measured using a home-built setup. The scheme of the setup and a detailed description can be found in the Supporting information. A Flame-EOP inductively coupled plasma optical emission spectrometer (ICP-OES) from Spectro (Germany) was used for the determination of the elemental composition of core and core–shell UCLNPs. The upconversion luminescence spectra from UCLNPs dispersions in cyclohexan were recorded with a luminescence spectrometer (LS 50 B) from PerkinElmer (UK), modified with a 980-nm CW laser (120 mW) from Roithner (Austria) for upconversion photo-excitation. The chemically modified enzyme GOx-FS was separated from the excess of FS using a low-pressure chromatography system. This system consisted of a glass column (13 cm long, 1 cm diameter) filled with Sephadex G-50. The eluent was supplied by a peristaltic pump Minipuls 3 from Gilson (USA). The end of the column was connected to a UV–vis spectrophotometer 8453A from Agilent (Germany). The poly(acrylamide) films were measured using the spectrofluorometer Quanta Master™ 40 from Photon Technology International (PTI, USA) equipped with a RLDH980-200-3 CW diode laser module, 980 nm, 200 mW, power density 25.5 W/cm² from Roithner (Austria). The FIA system consisted of a peristaltic pump Minipuls 3 from Gilson (USA) and 0.5 mm inner-diameter PTFE tubes. Furthermore, we used Amicon-Ultra 10 kDa centrifugal filters from Millipore (Germany) and a MiniSpin centrifuge from Eppendorf (Germany) for ultracentrifugation.

2.3. Synthesis of core nanoparticles: $NaYF_4$(25%Yb, 0.3%Tm)

Hexagonal-phase, lanthanide-doped $NaYF_4$ nanoparticles were prepared according to our previously reported procedure (Wilhelm et al., 2013). The salts of $YCl_3 \cdot 6H_2O$ (0.747 mmol), $YbCl_3 \cdot 6H_2O$ (0.25 mmol), and $TmCl_3 \cdot 6H_2O$ (0.003 mmol) were dissolved in approximately 5 mL of methanol by sonication. This solution was transferred into a 50 mL flask, mixed with 8 mL of oleic acid and 15 mL of 1-octadecene under an atmosphere of nitrogen and heated

to 160 °C. A homogeneous, clear solution was formed after 30 min at 160 °C under vacuum. The reaction mixture was then cooled to room temperature and 10 mL of methanol containing NaOH (0.25 M) and NH_4F (0.4 M) was added at once. The resulting colloid suspension was refluxed at approximately 325 °C for 15 min, after stirring for 30 min at 120 °C. The UCLNPs were precipitated by addition of approximately 20 mL of ethanol and isolated via centrifugation at a relative centrifugal force (RCF) of 1000*g* for 5 min. The pellet was washed several times by dispersing it in small amounts (approximately 0.5 mL) of chloroform and cyclohexane, then precipitating them by the addition of a large excess (approximately 15 mL) of ethanol and acetone. Finally, the purified UCLNPs were dispersed in 10 mL of cyclohexane and used for the subsequent synthesis of the shell. Composition is provided in Table S1.

2.4. Synthesis of core–shell nanoparticles: $NaYF_4$(25%Yb, 0.3%Tm) @$NaYF_4$

The synthesis of the un-doped hexagonal $NaYF_4$ shell was based on a modified procedure as reported by Qian and Zhang (2008). $YCl_3 \cdot 6H_2O$ (0.5 mmol) was dissolved in 5 mL of methanol by sonication and transferred into a 50 mL flask under nitrogen atmosphere. Oleic acid (8 mL) and 1-octadecene (15 mL) were added under stirring. The mixture was heated to 160 °C under vacuum. A homogeneous, clear solution was formed after 30 min. Afterwards, the reaction mixture was cooled to 90 °C. The whole amount of core-only UCLNPs (resulted from the synthesis described before) dispersed in 10 mL of cyclohexane was added under nitrogen atmosphere. This dispersion was stirred for additional 30 min at 90 °C in order to evaporate the cyclohexane. After cooling to room temperature, 5 mL of a methanol solution containing NaOH (0.25 M) and NH_4F (0.4 M) was added at once. The resulting colloid suspension was first heated to 120 °C and stirred for 30 min at this temperature and then heated to reflux (~325 °C for 20 min). The core–shell UCLNPs were precipitated by the addition of ~20 mL of ethanol and isolated via centrifugation at 1000*g* RCF for 5 min. The resulting pellet was washed several times by dispersing it in small amounts (~0.5 mL) of chloroform and cyclohexane, then precipitating them by the addition of a large excess (~15 mL) of ethanol and acetone. Finally, the purified UCLNPs were dispersed in 10 mL of cyclohexane and stored. The elemental composition of the core–shell UCLNPs is provided in Table S1.

2.5. Preparation of water dispersible core–shell UCLNPs (wdUCLNPs)

A general and universal method reported by Li et al. (2012) was used in order to get the initial hydrophobic (oleic acid-coated) UCLNPs dispersible in water media. In more detail, 1 mL of UCLNPs (~10 mg mL^{-1}) dispersion in cyclohexane was transferred to a 50 mL round bottom flask. Subsequently, the cyclohexane was evaporated and the UCLNPs dispersed again in 2 mL of chloroform. The DSPE-mPEG(2000) (5 μmol) dissolved in 2 mL of chloroform was added and the resulting mixture sonicated for 3 min at room temperature. The chloroform was subsequently evaporated, which resulted in the formation of a clear film on the bottom of the flask. This flask was incubated for 1 h at 60 °C under vacuum. Afterwards, the film was hydrated with 10 mL of MES buffer (0.1 M, pH 6). A clear dispersion of hydrophilic UCLNPs was obtained, which were coated with DSPE-mPEG(2000). The dispersion was purified by three steps of centrifugation (RCF 17,000*g* for 15 min) and subsequent redispersion in MES buffer solution (pH 6, 0.1 M). Finally, the DSPE-mPEG(2000)-coated UCLNPs were dispersed in 10 mL of MES buffer (approximately 1 mg mL^{-1}) and used for further incorporation in poly(acrylamide) films.

2.6. Preparation of chemically modified enzyme GOx-FS

The enzyme GOx was chemically modified by mixing 300 μL of carbonate solution (pH 8.5, 0.1 M) containing 20 mg of GOx with 200 μL of a solution of 6-[fluorescein-5(6)-carboxamido]hexanoic acid N-hydroxysuccinimide ester (FS) prepared by dissolving 2 mg of the solid in 1 mL of dimethyl sulfoxide. The mixture was allowed to react in the dark at room temperature for 90 min. The excess of FS was then separated using the chromatographic system described in the instrumentation part. We used MES buffer solution (pH 6, 0.1 M) as an eluent at a flow rate of 1.5 mL/min. The first fraction, which absorbed at 280 nm and 470 nm, contained the chemically modified enzyme GOx-FS and was recovered. The second fraction contained the excess of FS and was discarded.

2.7. Preparation of poly(acrylamide) films containing GOx-FS and wdUCLNPs

Poly(acrylamide) films with various thicknesses (from 4.0 to 0.8 mm) and various concentrations of wdUCLNPs (from 0.13 to 2.8 mg mL^{-1}) and GOx-FS (from 400 to 1880 U mL^{-1}) were prepared. We dissolved 75 mg of acrylamide and 5 mg of N,N′-methylenebisacrylamide in 500 μL of the corresponding GOx-FS/wdUCLNPs mixture (Ortega et al., 2013). Subsequently, 4 μL of ammonium persulfate solution (10% w/v) was added and the dissolved oxygen was removed by bubbling nitrogen through the solution. Finally, 0.5 μL of TEMED was added and the mixture was immediately spread on a glass cast ($0.7 \times 0.5 \times 4 - 0.8$ mm). The mixture was left to react for one hour, after being covered with a glass slide. The sensor film was washed several times with MES buffer solution (pH 6, 0,1 M) before being used.

2.8. Measurement system and optical setup

UCLNPs emit fluorescence at several wavelengths (Figs. S3 and S4). Some of them change during the enzymatic reaction but others, at the fluorescence 645 nm, do not. We use this fact to improve the precision of the measurements using the fluorescence intensity at 645 nm (F_{645}) as a reference. To do that the fluorescence intensity at the working wavelength (F_λ) is divided by F_{645}.

A home-made flow cell (Fig. S5), which was incorporated in an FIA system, was used for the fluorescence measurements. The sensor film was placed in the hole of the stainless steel piece and covered with two windows for providing optical transparency, which was held with Hoffmann clamps. The flow cell was fixed in the sample compartment of the spectrofluorometer between quartz excitation and emission lenses. A diode laser (CW, 980 nm, 200 mW, 25.5 W/cm²) was used as excitation source, at 180°, instead of the xenon arc lamp of the spectrofluorometer, which was previously blocked. Both UCLNPs emission and harmonic of the laser excitation produced by the emission monochromator (490 nm) were collected by the detector of the spectrofluorometer. During the measurements, the MES buffer solution (pH 6, 0.1 M) flowed across the cell at 0.5 mL/min and the fluorescence intensity was simultaneously monitored at 520 nm and at a reference wavelength of 645 nm. Different volumes (0.5, 1 or 1.5 mL) of various glucose concentrations were injected for the optimization of the injection volume. The area (A) and the height (H) of the quotient signal were used as the analytical parameters.

3. Results and discussion

3.1. Choice of materials for the synthesis of UCLNPs

The UCLNPs are capable of converting NIR light into visible light. The host material of the core UCLNPs consists of hexagonal-phase

$NaYF_4$, which is doped with 25 mol% of Yb^{3+} and 0.3 mol% of Tm^{3+} ions. They were prepared following an optimized bottom-up approach (Wilhelm et al., 2013). In Fig. 2A the TEM image of the roughly spherical core UCLNPs is shown. The nanoparticles possess an average diameter of 26.0 nm (revealed from TEM images) with a standard deviation of 0.5 nm (Fig. 2D). The hydrodynamic diameter of these UCLNPs dispersed in cyclohexane is 31 nm with a PdI (polydispersity index) of 0.062 (see Dynamic Light Scattering measurements in Fig. S6). The average diameter evaluated from the XRD experiments using the well-established *Scherrer* equation (Boyer et al., 2006) is about 26 nm, which is in good coincidence to the results from the TEM image.

It is reported that a shell based on $NaYF_4$ enhances significantly the upconversion efficiency of the lanthanide-doped UCLNPs core (Yi and Chow, 2006). Boyer et al. measured an increase of absolute quantum yield of 300% after the growth of a $NaYF_4$ shell over Yb/Er-doped core UCLNPs (30 nm in diameter). The quantum yield for the Yb/Er-doped core UCLNPs without shell is $0.10 \pm 0.05\%$ (Boyer and van Veggel, 2010). We used a modified protocol based on a heat-up method as reported by Qian and Zhang (2008) for the synthesis of the $NaYF_4$ shell. In detail, the pre-synthesized β-phase UCLNPs act as seeds/nuclei for a seed-mediated shell growth. The TEM image of the rod-like core–shell UCLNPs is shown in Fig. 2B. From this fact one can conclude that a non-centrosymmetric shell of $NaYF_4$ is formed around the core UCLNPs and that there is a preferred growth in one crystallographic direction (Johnson and Veggel, 2013). The TEM image does not allow discriminating between core and shell, since both mainly consist of $NaYF_4$. Nevertheless, there is an indirect evidence for the formation of a core–shell structure. First, the size of the UCLNPs increased significantly after the shell growth, which is evaluated in Fig. 2D and E. Second, the upconversion luminescence enhancement provides further confirmation for the core–shell structure, since a $NaYF_4$ shell is known to shield the core from surface and solvent quenching (Johnson et al., 2012). The XRD patterns shown in Fig. 2F prove the hexagonal crystal structure of both the core and the core–shell UCLNPs.

3.2. Spectra and luminescence decay times of UCLNPs

We proved the enhancement of the upconversion efficiency by the determination of the upconversion intensity and luminescence lifetime of UCLNPs dispersed in cyclohexane (see Supporting information: UCLNP luminescence spectra and luminescence lifetimes of UCLNP). The upconversion intensity at 475 nm is about 61 times stronger for the core–shell UCLNPs as compared to the core-only UCLNPs dispersed in cyclohexane. We normalized the

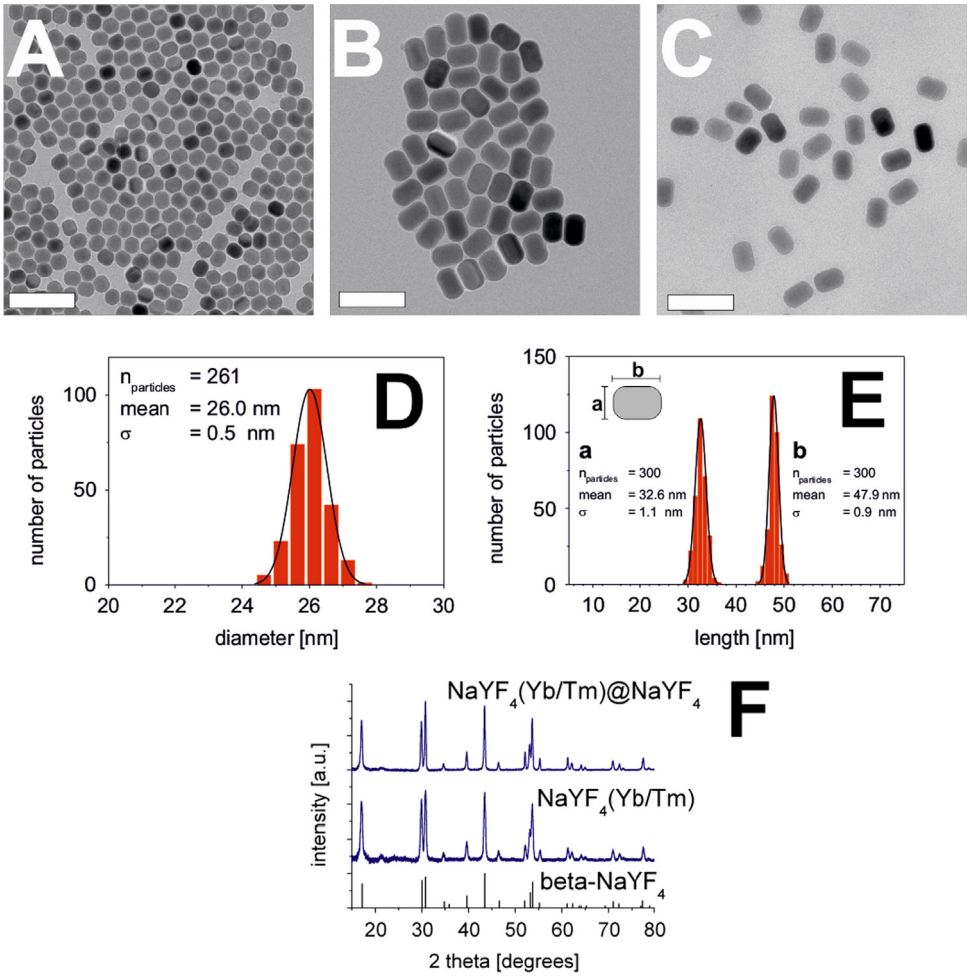

Fig. 2. TEM images of core $NaYF_4$(25%Yb,0.3%Tm) UCLNPs (A), core–shell $NaYF_4$(25%Yb,0.3%Tm)@$NaYF_4$ UCLNPs (B), and DSPE-mPEG(2000)-coated $NaYF_4$(25%Yb,0.3%Tm)@$NaYF_4$ wdUCLNPs (C). Scale bar: 60 nm. The size histograms revealed from the TEM images of the core $NaYF_4$(25%Yb,0.3%Tm) UCLNPs (D), and the core–shell $NaYF_4$(25%Yb,0.3%Tm)@$NaYF_4$ UCLNPs (E) are shown. One should note that in (D) the diameter of the roughly spherical core UCLNPs is displayed. However, in (E) the two dimensions (a, b) of the rod-like core–shell UCLNPs are evaluated. Graph (F) shows the corresponding XRD patterns, which are compared with the standard XRD pattern for β-$NaYF_4$ (ICDD PDF 16-334).

upconversion luminescence intensity to an equal Yb^{3+} concentration as obtained by ICP-OES measurements. The average upconversion luminescence lifetime was determined for the blue and red region (see Supporting information: Luminescence lifetimes of UCLNP). It is worth noting that two lifetimes (0.4 and 0.6 ms) can be calculated for the core UCLNPs in the blue range. The upconversion luminescence lifetime for the core–shell UCLNs in this region is 0.9 ms. The average lifetime in the red range increased from 0.6 ms for the core UCLNPs to 1.5 ms for the core–shell UCLNPs dispersed in cyclohexane because of less non-radiative processes by interaction with solvent molecules. The increase in size and upconversion luminescence lifetimes of the UCLNPs as well the enhancement of the UCLNPs intensities after shell growth taken together provide evidence for the formation of a core–shell homoepitaxial structure.

3.3. UCLNPs surface modification

The UCLNPs are capped with oleic acid after synthesis and therefore can only be dispersed in organic solvents. In order to work in a biosensing scheme, it is imperative to transfer the oleic acid-capped UCLNPs into an aqueous medium. We used a phospholipid (DSPE-mPEG2000) that can act as an amphiphilic ligand. The DSPE-mPEG2000 contains three segments: two fatty acid chains (stearic acid), a phosphate group, and a poly(ethylene glycol) moiety. The hydrophobic van-der-Waals interactions between the oleic acid ligands on the UCLNPs surface and the hydrophobic tails of the phospholipids render the UCLNPs water-dispersible, since the hydrophilic segment of the phospholipids points out towards the aqueous environment (Li et al., 2012). Fig. 2C shows a TEM image of hydrophilic UCLNPs dispersed in MES buffer (0.1 M, pH 6.0). The DSPE-mPEG2000-coated UCLNPs form a transparent colloidal dispersion (concentration approximately 1 mg mL^{-1}), which is stable for several weeks without any noticeable precipitation.

3.4. Sensing schemes and analytical signal

The emission spectrum of UCLNPs displays two maxima; a smaller one at 450 nm, and a more intense maximum at 475 nm (Fig. 3). This blue upconversion luminescence overlaps the absorption of FAD and $FADH_2$ (Fig. 3, left) and the excitation spectrum of GOx-FS (Fig. 3, right). According to these spectra, there are two possibilities for coupling the upconversion fluorescence of UCLNPs to the enzyme in order to design an optical (bio)sensor.

The first one corresponds to the use of unmodified GOx. In this case, since the molar absorptivity of $FADH_2$ is lower than that of FAD at the UCLNPs fluorescence, a change in the inner filter effect should be observed throughout the reaction, the change being related to the glucose concentration. This methodology was assayed and optimized. A mathematical model was developed relating the upconversion luminescence with GOx and glucose concentration and it was demonstrated that the change in the inner filter was the responsible of the signal. However, low sensitivity and a small linear response range were obtained. All these results are shown in Supporting information (see Results obtained using unmodified GOx).

We therefore chose a second strategy that is based on the finding that fluorescein-labeled GOx (GOx-FS) shows an emission at 520 nm (due to FS fluorescence) upon 490 nm excitation which changes on enzymatic oxidation of glucose (Sanz et al., 2003). This change can be related to the glucose concentration (see Supporting Information: GOx-FS as a glucose biosensor). As shown in Fig. 1, the methodology used depicts that both FAD and FS absorb the radiation emitted by the UCLNPs and the fluorescence from FS is observed (F_a); the GOx and the UCNP concentrations can be higher enough for supporting this mechanism; however, additional effects could also favor the whole process (see Supporting information: considerations about the mechanism). After glucose addition, since $FADH_2$ absorbs less than FAD, the FS absorption increases and therefore its fluorescence (F_b). The analytical advantage of using GOx-FS is not only the longer wavelength (poly (acrylamide) films are more transparent at 520 nm) but also the higher ratios F_a/F and F_b/F, which provide a higher measurement precision. Previous studies were carried out using UCLNPs and GOx-FS in solution with good results and later were incorporated in polyacrylamide (PAA) films.

Fig. 4 shows that the UCLNPs indeed act as nanolamps. Studies were performed using wdUCLNP and GOx-FS incorporated in PAA films. The sensor films (thickness 0.8 mm) containing 2.8 mg mL^{-1} UCLNPs with various amounts of GOx-FS display luminescence >500 nm upon 980 nm CW laser excitation. The emission intensity increases along with the concentration of GOx-FS. From these results we conclude that both, FAD and FS, absorb the upconversion luminescence emitted by the UCLNPs upon 980 nm CW laser excitation.

The injection of solutions of different glucose concentrations (1 mL) in the biosensor (sensor film 2 mm thickness, [wdUCLNPs]= 0.9 mg mL^{-1}, [GOx-FS] =400 U mL^{-1}), under the working conditions indicated in Section 2.8, gave transient signals (Fig. S12) whose areas (A) and heights (H) were related to the analyte concentration. Fig. S13 shows that H and log A linearly change with glucose concentration [G_0].

3.5. Chemical parameter optimization

With the aim of improving the analytical signals obtained, the amount of wdUCLNPs in films was first optimized. Sensor films (0.8 mm thickness) having the same concentration of GOx-FS (400 U mL^{-1}) and different concentrations of wdUCLNPs (3.6, 2.8, 0.84 and 0.13 mg mL^{-1}) were prepared and different volumes

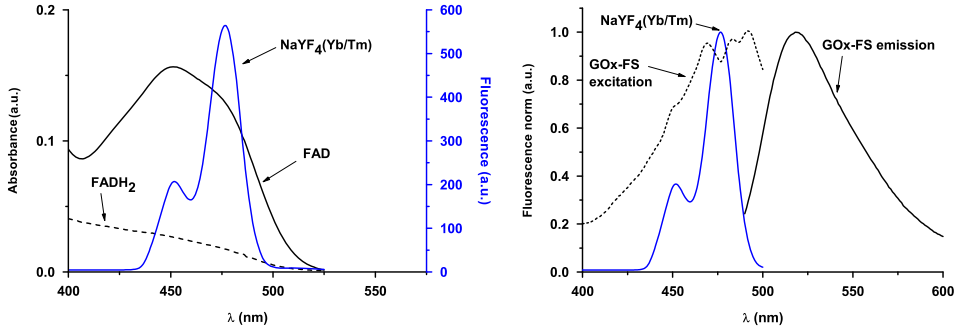

Fig. 3. Normalized absorption spectra of FAD and $FADH_2$ in GOx (left). Normalized excitation and emission spectra of GOx-FS (right). Both graphs contain the luminescence spectrum of UCLNPs upon 980 nm laser excitation (15 W/cm^2, solid blue line). (For interpretation of the references to color in this figure legend, the reader is referred to the web version of this article.)

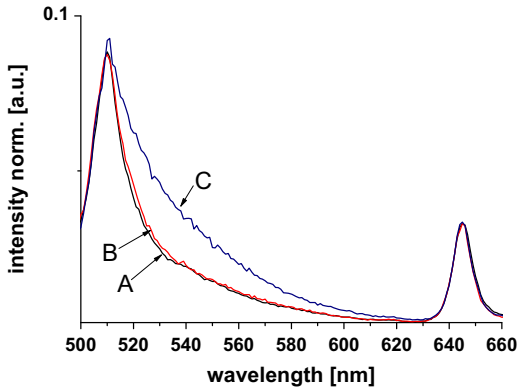

Fig. 4. Normalized emission spectra of various GOx-FS concentrations (400 U mL^{-1} A, 810 U mL^{-1} B, and 1880 U mL^{-1} C) embedded in a sensor film (thickness 0.8 mm) containing 2.8 mg mL^{-1} UCLNPs upon 980 nm CW laser excitation (25.5 W/cm^2).

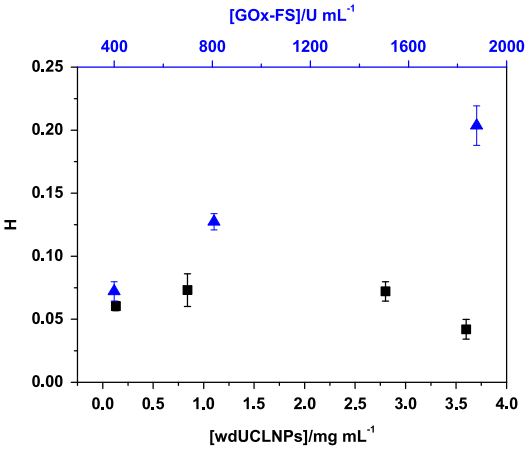

Fig. 5. Height values obtained after 1 mL injections of a 6.6 mM glucose solution (thickness of the film: 0.8 mm). ▲ Different GOx-FS concentrations in films containing [wdUCLNPs]=2.8 mg mL^{-1}. ■ Different wdUCLNPs concentrations in films containing [GOx-FS]=400 U mL^{-1}.

of a solution of glucose (6.6 mM) were injected. The height average values (3 measurements) corresponding to 1 mL injected are shown in Fig. 5 (for higher and lower volumes, and for areas see Fig. S14). It is well known that fluorescence intensity increase by the power of the excitation source, so it should be expected that the sensitivity would increase with the UCLNPs concentration. However, the results indicate that an optimum zone is obtained. This optimum can be justified because the PAA films structure changes with UCLNPs and this limit the GOx-FS entrapment capacity. Since the results also indicate that the noise of the signals decrease as the amount of nanoparticles increase (Table S6), this amount should be kept as high as possible in the plateau zone. This finding is very important for this methodology and could be taken into account when other solid supports are being tested.

Furthermore, sensor films containing the optimal wdUCLNPs concentration (2.8 mg mL^{-1}) and different GOx-FS concentrations (400, 810 and 1080 U mL^{-1}) were prepared in order to optimize the GOx-FS concentration in the film. The *A* and *H* values obtained after the injection of 1 mL of glucose (6 mM) are shown in Fig. 6 (see Fig. S15 for 0.5 mL). The results indicate that the signal increases with the concentration of GOx-FS. We should hope linear increases, but as indicated before, the higher the GOx-FS amount entrapped the lower the amount of wdUCLNP, so the excitation intensity diminishes.

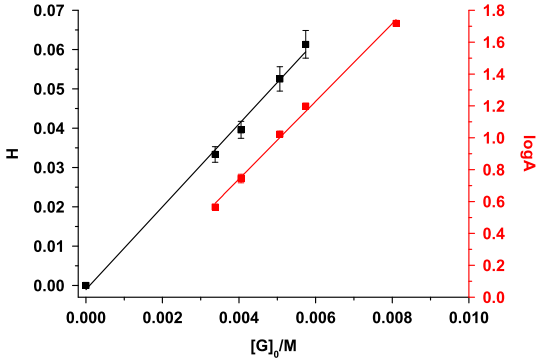

Fig. 6. Height and logarithm of area vs. glucose concentration calibration plots at optimal conditions. Sensor film: [wdUCLNPs] =2.8 mg mL^{-1}, [GOx-FS]=1880 IU mL^{-1}, 0.8 mm thickness. Volume injected: 1 mL. Working conditions indicated in 2.8. (Error bars for log *A* are very low and are hardly observed in the representation.)

3.6. Physical parameters optimization: stop flow conditions

Films with different thicknesses were tested (0.8, 2 and 4 mm). The obtained results indicated that the higher the thickness the higher the signals; however 4 and 2 mm thicknesses involved some difficulties concerning the fluorescence measurements. Because of the low volume of buffer solution flowing inside the cell, heating produced by the laser illumination is not transferred and removed efficiently. This leads to the sensor film warming and the consequent fluorescence drift (see Table S7). In order to minimize this issue, the sensor film thickness was reduced to 0.8 mm.

The influence of the sample volume (injection volume) was also studied. Actually, some of the optimization studies presented below were performed using different volumes (Figs. S14 and S15) and they allow to get some conclusions. It is clear from these graphs that the higher the volume, the higher the signal, but those results do not shows that the width in term of time of the transient signal also increases; so, widths of 200, 500 and 1000 s were obtained injecting 0.5, 1 and 1.5 mL sample (for 6.6 mM glucose) respectively. These results show that the sensitivity can be increased but at the expenses of increasing reaction time.

Several tests were carried out in stop flow, i.e. the sample completely fills the flow cell and the reaction is left to completion. Under those conditions the fluorescence intensity increases until a plateau is obtained, its *H* (H_{sf}) being proportional to the glucose concentration. This value is important because as we are working in flow injection mode, the H_{sf} represents the maximum value which could be expected, i.e. the maximum sensitivity we can obtain. Fig. S16 compares theses results and permits to conclude that 1.5 mL volume is nearly the maximum volume which can be injected in order to increase the sensitivity.

3.7. Analytical figures of merit

Calibration graphs were obtained under the best conditions considered (0.8 mm film thickness, [wdUCLNPs]=2.8 mg mL^{-1}, [GOx-FS] =1880 IU mL^{-1}) but using 1 mL glucose volume, working in both, *H* and *A*. The experimental results are shown in Fig. S17. As can be seen, also under the UCLNP and GOx-FS optimal conditions *H* linearly increases with the glucose concentration ($H=10.54\ [G]_0-1.06.10^{-3}$; $R^2=0.994$) In all cases the relative standard deviations (RSD) obtained were better than 6%.

Regarding the area, in agreement with the previous results (Section 3.4), the relationship between *A* and the glucose concentration is not linear. A mathematical explanation is given in Supporting information (Fig. S19). A linearity between log *A* and analyte concentration was

obtained ($\log A = 243.7\ [G]_0 - 2.332 \times 10^{-1}$; $R^2 = 0.9999$) and the RSD were even better than with the H (about 4%). The sensitivity and the linear response range shown for this sensor are of the same order than that obtained in the absence of wdUCLNPs (Sanz et al., 2003).

A very first evaluation of the lifetime of the sensor film was performed. 0.5 mL of a solution of glucose (6.6 mM) was injected on different days. A film (0.8 mm thickness) containing 5.6 mg mL^{-1} of wdUCLNPs and 400 U mL^{-1} of GOx-FS was used and areas and heights obtained are shown in Table S8. When not measured, the sensor film was stored in MES buffer at 4 °C.

4. Conclusions

This work demonstrates how the UCLNPs can be used as nanolamps in combination with the spectroscopic properties of fluorescent dyes of modified enzymes. The NIR excitation of UCLNPs is of major advantage, since pretreatment of biological samples is not needed and auto-fluorescence is greatly reduced. The combination of UCLNPs with GOx-FS can be considered as a new approach for the development of new sensing scheme for continuous monitoring of glucose concentration in the whole blood. Furthermore, this sensor concept has a large scope and can be extended to the determination of other biochemical metabolites (e.g., cholesterol and choline) after replacing the GOx by the corresponding flavoenzyme.

Acknowledgments

The authors thank the MINECO of Spain (Projects CTQ2012-34774 and CTQ2012-35535) and the Gobierno de Aragón (DGA-FEDER) for the financial support. M. del Barrio thanks the CSIC for the funding for her PhD (JAE-Pre contract). Stefan Wilhem thanks the DFG for funding (ERA Chemistry project: WO609/12-1).

Appendix A. Supporting information

Supplementary data associated with this article can be found in the online version at http://dx.doi.org/10.1016/j.bios.2014.02.076.

References

Auzel, F., 2004. Chem. Rev. 104, 139–173.
Boyer, J.-C., van Veggel, F.C.J.M., 2010. Nanoscale 2 (8), 1417–1419.
Boyer, J.-C., Vetrone, F., Cuccia, L.A., Capobianco, J.A., 2006. J. Am. Chem. Soc. 128 (23), 7444–7445.
Chan, E.M., Han, G., Goldberg, J.D., Gargas, D.J., Ostrowski, A.D., Schuck, P.J., Cohen, B.E., Milliron, D.J., 2012. Nano Lett. 12 (7), 3839–3845.
Cheng, L., Wang, C., Liu, Z., 2013. Nanoscale 5 (1), 23–37.
De Luca, P., Lepore, M., Portaccio, M., Esposito, R., Rossi, S., Bencivenga, U., Mita, D., 2007. Sensors 7 (11), 2612–2625.
Galban, J., Sanz-Vicente, I., Ortega, E., del Barrio, M., de Marcos, S., 2012. Anal. Bioanal. Chem. 402 (10), 3039–3054.
Gorris, H.H., Wolfbeis, O.S., 2013. Angew. Chem. Int. Ed. 52 (13), 3584–3600.
Haase, M., Schafer, H., 2011. Angew. Chem. 50 (26), 5808–5829.
Jin, S., Veetil, J.V., Garrett, J.R., Ye, K., 2011. Biosens. Bioelectron. 26 (8), 3427–3431.
Johnson, N.J., Veggel, F.J.M., 2013. Nano Res. 6 (8), 547–561.
Johnson, N.J.J., Korinek, A., Dong, C., van Veggel, F.C.J.M., 2012. J. Am. Chem. Soc. 134 (27), 11068–11071.
Kao, Y.-T., Saxena, C., He, T.-F., Guo, L., Wang, L., Sancar, A., Zhong, D., 2008. J. Am. Chem. Soc. 130 (39), 13132–13139.
Li, L.-L., Zhang, R., Yin, L., Zheng, K., Qin, W., Selvin, P.R., Lu, Y., 2012. Angew. Chem. Int. Ed. 51 (25), 6121–6125.
Menyuk, N., Dwight, K., Pierce, J.W., 1972. Appl. Phys. Lett. 21 (4), 159–161.
Ortega, E., de Marcos, S., Galban, J., 2013. Biosens. Bioelectron. 41, 150–156.
Park, Y.I., Kim, J.H., Lee, K.T., Jeon, K.-S., Na, H.B., Yu, J.H., Kim, H.M., Lee, N., Choi, S.H., Baik, S.-I., Kim, H., Park, S.P., Park, B.-J., Kim, Y.W., Lee, S.H., Yoon, S.-Y., Song, I.C., Moon, W.K., Suh, Y.D., Hyeon, T., 2009. Adv. Mater. 21 (44), 4467–4471.
Qian, H.-S., Zhang, Y., 2008. Langmuir 24 (21), 12123–12125.
Sanz, V., Galban, J., De Marcos, S., Castillo, J.R., 2003. Talanta 60 (2–3), 145–423.
Shen, J., Zhao, L., Han, G., 2013. Adv. Drug Deliv. Rev. 65 (5), 744–755.
Silva, E., Edwards, A.M., 2006. Flavins Photochemistry and Photobiology. RSC, Cambridge, UK
Steiner, M.-S., Duerkop, A., Wolfbeis, O.S., 2011. Chem. Soc. Rev. 40 (9), 4805–4839.
Tatsu, Y., Yamamura, S., 2002. J. Mol. Catal. B 17 (3–5), 203–206.
Tuchin, V.V., 2009. Handbook of Optical Sensing of Glucose in Biological Fluids and Tissues. Taylor & Francis/CRC Press, Boca Raton, Fl, USA.
Wang, F., Banerjee, D., Liu, Y., Chen, X., Liu, X., 2010a. Analyst 135 (8), 1839–1854.
Wang, F., Han, Y., Lim, C.S., Lu, Y., Wang, J., Xu, J., Chen, H., Zhang, C., Hong, M., Liu, X., 2010b. Nature 463 (7284), 1061–1065.
Wang, F., Liu, X., 2009. Chem. Soc. Rev. 38 (4), 976–989.
Weidemaier, K., Lastovich, A., Keith, S., Pitner, J.B., Sistare, M., Jacobson, R., Kurisko, D., 2011. Biosens. Bioelectron. 26 (10), 4117–4123.
Wilhelm, S., Hirsch, T., Patterson, W.M., Scheucher, E., Mayr, T., Wolfbeis, O.S., 2013. Theranostics 3 (4), 239–248.
Wu, S., Han, G., Milliron, D.J., Aloni, S., Altoe, V., Talapin, D.V., Cohen, B.E., Schuck, P.J., 2009. Proc. Natl. Acad. Sci. USA 106 (27), 10917–10921.
Xu, C.T., Zhan, Q., Liu, H., Somesfalean, G., Qian, J., He, S., Andersson-Engels, S., 2013. Laser Photonics Rev. 7 (5), 663–697.
Ye, X., Collins, J.E., Kang, Y., Chen, J., Chen, D.T.N., Yodh, A.G., Murray, C.B., 2010. Proc. Natl. Acad. Sci. USA 107 (52), 22430–22435.
Yi, G.-S., Chow, G.-M., 2006. Chem. Mater. 19 (3), 341–343.